



# ESA CONTRACT REPORT

Contract Report to the European Space Agency

## **SMOS Operational Emergency Services - Floods**

*Authors: Calum Baugh, Patricia de  
Rosnay and Heather Lawrence*

Report for ESA contract 4000125399/18/I-BG

Technical Report 3 (TR3) Work Package Floods-1  
(addendum TH1-020)

**European Centre for Medium-Range Weather Forecasts  
Europäisches Zentrum für mittelfristige Wettervorhersage  
Centre européen pour les prévisions météorologiques à moyen terme**



Series: ECMWF - ESA Contract Report

A full list of ECMWF Publications can be found on our web site under:

<http://www.ecmwf.int/publications/>

© Copyright 2019

European Centre for Medium Range Weather Forecasts  
Shinfield Park, Reading, RG2 9AX, England

Literary and scientific copyrights belong to ECMWF and are reserved in all countries. This publication is not to be reprinted or translated in whole or in part without the written permission of the Director General. Appropriate non-commercial use will normally be granted under the condition that reference is made to ECMWF.

The information within this publication is given in good faith and considered to be true, but ECMWF accepts no liability for error, omission and for loss or damage arising from its use.

Contract Report to the European Space Agency

## **SMOS Operational Emergency Services - Floods**

*Authors: Calum Baugh, Patricia de Rosnay and  
Heather Lawrence*

*Draft report for ESA contract 4000125399/18/I-BG*

European Centre for Medium-Range Weather Forecasts  
Shinfield Park, Reading, Berkshire, UK

August 2019



## TABLE OF CONTENTS

<b>Abbreviations</b> .....	<b>ii</b>
<b>1. Introduction</b> .....	<b>1</b>
<b>2. Description of IFS SMOS Data Assimilation Experiment</b> .....	<b>3</b>
<b>3. Description of GloFAS Experiments</b> .....	<b>3</b>
<b>4. Streamflow Verification Methodology</b> .....	<b>4</b>
<b>5. Verification Results</b> .....	<b>5</b>
5.1. Verification against Observed Streamflow .....	5
5.1.1. United States .....	5
5.1.2. Australia.....	10
5.2. Verification against GloFAS ERA-5 Simulation.....	15
<b>6. Discussion &amp; Conclusions</b> .....	<b>21</b>
<b>Acknowledgements</b> .....	<b>22</b>
<b>References</b> .....	<b>22</b>

## Abbreviations

ECMWF	.....	European Centre for Medium-range Weather Forecasts
CEMS	.....	Copernicus Emergency Management Service
DEM	.....	Digital Elevation Model
EA	.....	Evolutionary Algorithm
EPSG	.....	European Petroleum Survey Group
EWS	.....	Early Warning System
FAO	.....	United Nations Food and Agriculture Organization
GloFAS	.....	Global Flood Awareness System
GRDC	.....	Global Runoff Data Centre
GWD-LR	.....	Global Width Database for Large Rivers
HTESSEL	.....	Hydrology Tiled ECMWF Scheme for Surface Exchanges over Land
HydroSHEDS	.....	Hydrological data and maps based on Shuttle Elevation Derivatives at multiple Scales
IFS	.....	Integrated Forecast System
JRC	.....	European Commission Joint Research Centre
KEGE	.....	Kling-Gupta Efficiency
LDAS	.....	Land Data Assimilation Scheme
LSM	.....	Land Surface Model
QC	.....	Quality Control
SEKF	.....	Simplified Extended Kalman Filter
SMOS	.....	Soil Moisture and Ocean Salinity
SRTM	.....	Shuttle Radar Topography Mission
VIC	.....	Variable Infiltration Capacity

## Abstract

In this study the impacts of the data assimilation of the SMOS soil moisture neural network trained on ECMWF product upon streamflow estimates were investigated. Two hydrological experiments were performed, one which used hydro-meteorological forcings produced with the assimilation of the SMOS data, the other using forcings which excluded the assimilation of the SMOS data. Both hydrological simulations produced streamflow estimates using the Global Flood Awareness System [GloFAS], run at ECMWF on behalf of the European Commission Copernicus Emergency Management Service. Both sets of experiment results were verified against streamflow observations in the United States and Australia, and were also analysed globally with respect to a GloFAS simulation forced with ERA-5 re-analysis which provided a benchmark acting as global proxy observations. Skill scores were computed for each experiment against the observation datasets, the differences in the skill scores were used to identify where hydrological skill may be affected by the assimilation of SMOS soil moisture data. Results found that skill score differences between the two GloFAS data assimilation experiments were pronounced within a tropical band of latitude. Differences were also present in areas such as south east Asia and the Himalayas. There was no clear spatial trend to these differences, so it is not possible to conclude whether a particular region's hydrological skill is improved by the assimilation of SMOS soil moisture. Investigating the differences between the simulations at individual gauging stations found that they often only occurred during a single flood event, for the remainder of the simulation period the experiments were almost identical. Future work could further understand the impact of SMOS soil moisture data assimilation by focussing the analysis on individual flood events and correlating any differences to the analysis increments. Therefore it is not possible to conclude whether the assimilation of SMOS soil moisture improves the hydrological skill of GloFAS streamflow predictions. However the assimilation may affect individual flood peaks but further analysis is required.

## 1. Introduction

As part of the European Commission Copernicus Emergency Management Service [CEMS] for floods, the European Centre for Medium Range Weather Forecasts [ECMWF] operates the Global Flood Awareness System [GloFAS]. This provides once daily [00 UTC] forecasts of streamflow globally at  $0.1^\circ$  spatial resolution and daily temporal resolution up to 46 days ahead.

Streamflow forecasts are produced by coupling the surface and subsurface runoff forecasts from the ECMWF Integrated Forecast System [IFS] with the kinematic channel routing procedure within the LISFLOOD hydrological model. The coupling is necessary because no lateral routing of runoff exists within the IFS.

Within IFS the surface and subsurface runoff are calculated from the Hydrology Tiled ECMWF Scheme for Surface Exchanges of Land [HTESSEL] land surface model [LSM]. The soil water budget in HTESSEL is computed at each computational node using the Richards equation of water flow through the unsaturated soil profile. At the top boundary layer water enters the soil as precipitation minus evaporation and runoff and at the bottom boundary layer water exits as free draining. The soil hydraulic conductivity is calculated from the van Genuchten equation which is a function of pressure head which in turn relates to the soil texture. Different parameters are assigned to each soil texture class derived from the Food and Agriculture Organization [FAO] dataset. The saturated hydraulic conductivity is used to calculate the maximum infiltration rate which is then used to calculate the amount of runoff. Runoff is

generated in a Hortonian manner when the throughfall plus the snowmelt exceeds the maximum infiltration rate.

Each forecast from the IFS is initialised from the ECMWF analysis fields. The analysis is produced by assimilating the first guess [i.e. the previous forecast] with the latest near real time hydro-meteorological observations. The Land Data Assimilation Scheme [LDAS] of the IFS includes an analysis of soil moisture, which combines a two-dimensional screen level analysis of 2 metre temperature and relative humidity observations from SYNOP with soil moisture observations from satellite sensors. A Simplified Extended Kalman Filter [SEKF] is used to analyse the soil moisture state vector for each grid point at each time step [de Rosnay *et al.*, 2013]. A more detailed description of the soil moisture data assimilation procedure can be found in the IFS documentation [ECMWF, 2018]. Currently satellite soil moisture observations from the Advanced Scatterometer satellite [ASCAT] and SMOS [since model cycle 46r1 released 12<sup>th</sup> June 2019] are used within the LDAS soil moisture procedure. Therefore the assimilation of the SMOS soil moisture observations may have an impact upon the hydrological forecasting from the HTESSSEL LSM.

GloFAS produces global ensemble streamflow forecasts. It has been run at ECMWF since 2011 and has been operational since 23<sup>rd</sup> April 2018. It routes the forecasted surface runoff from HTESSSEL along a one-dimensional channel network using a kinematic solution of the St. Venant equations [van der Knijff *et al.*, 2010]. Calculating this requires information about the channel length, gradient, flow width and depth as well as the Manning's roughness coefficient. This information is obtained firstly from the global river network database [Wu *et al.*, 2012], which includes a river channel network at 0.1° spatial resolution from the Digital Elevation Model [DEM] created by the HydroSHEDS project [Lehner *et al.*, 2008]. This is a hydrologically conditioned version of the original Shuttle Radar Topography Mission [SRTM] DEM to ensure continuous stream networks. River widths are obtained from the Global Width Database for Large River [GWD-LR, Yamazaki *et al.*, 2014]. Bankfull water depth was estimated using the Manning's equation applied to long term average discharge observations.

GloFAS also includes 463 large lakes and 667 reservoirs whose locations and attributes were obtained from global datasets [Zajac *et al.*, 2017]. The outflow from each lake is computed using the relationship with lake level using the weir equation [Bollrich, 1992]. The extraction of water through irrigation is represented by subtracting from the forecasted streamflow a value taken from a monthly climatology [Hirpa *et al.*, 2018]. Finally, open water evaporation is estimated using the Penman-Monteith with forcings taken from IFS variables.

Eight of the GloFAS model parameters were tuned in a recent calibration exercise, including the channel Manning's  $n$ , the multiplier for lake outflow and flood storage and outflow for reservoirs [Hirpa *et al.*, 2018]. An Evolutionary Algorithm [EA] was used with the Kling-Gupta Efficiency metric [KGE] calculated for streamflow as the objective function. The calibration was performed in 1,287 catchments ranging from 484 km<sup>2</sup> to 4,800,000 km<sup>2</sup> in size. At each station at least four years of observed daily streamflow data between 1995-2015 were required, these were mostly sourced from the Global Runoff Data Centre [GRDC]. The four-year observation sample was split into two years for calibration and two for validation. Within the former the calibration was performed using a maximum of 15 generations of the EA algorithm. Forcings of surface and subsurface runoff were obtained from the ECMWF IFS HTESSSEL reforecasts between 1995-2015 which were a combination of model cycles 41r1 and 41r2. Results from the calibration found improved streamflow estimation skill in 67% of the 1,287 catchments

[77% when excluding North America] [Hirpa *et al.*, 2018]. The skill improvement was lowest where there were large negative biases in the baseline simulations, which could be caused by precipitation underestimation [Hirpa *et al.*, 2018]. For catchments which were not part of the calibration exercise, default parameter values taken from the literature were used.

As described above, since ECMWF IFS model cycle 46r1 the surface and subsurface runoff forecasts from HTESSEL benefit from the assimilation of SMOS soil moisture observations. Since these forecasts are used to force the GloFAS model forecasts of streamflow, it therefore stands that these may also benefit from SMOS. To date however this potential benefit has not been investigated. Therefore the rest of this report describes the results of a data denial experiment to assess the sensitivity of GloFAS streamflow skill to the assimilation of SMOS within the IFS.

## 2. Description of IFS SMOS Data Assimilation Experiment

Two IFS simulations were performed to assess the role of SMOS data assimilation. One simulation included SMOS soil moisture data assimilation and the other excluded it. The simulations were run from 1<sup>st</sup> March 2017 to the 21<sup>st</sup> May 2018 using model cycle 45r1 with grid TCo399 [approximately 0.25°x0.25° horizontal resolution] and climate v015.

The SMOS soil moisture data used in this experiment were similar to that from the neural network processor used for preliminary offline data assimilation experiments conducted by [Rodríguez-Fernández *et al.*, 2019]. It was created by training SMOS dual-polarisation multi-angular level 1 brightness temperature measurements against ECMWF soil moisture analysis fields. However, for this study, the neural network product was trained on the ECMWF operational soil analysis instead of on the offline model soil moisture. In addition, data assimilation experiments were conducted in the IFS instead of the offline land surface model. So, they rely on coupled modelling and coupled assimilation approaches, and use a 12h assimilation window instead of 24h in the offline system. The SMOS IFS data assimilation experiments used in this report were also used to support the operational implementation of the SMOS NN product assimilation in IFS cycle 46r1 in June 2019 [de Rosnay *et al.*, 2019].

## 3. Description of GloFAS Experiments

The GloFAS suite was run using each of the aforementioned IFS experiments. The following output variables from the IFS experiments were used as forcings within GloFAS: *total precipitation, surface runoff, subsurface runoff, surface net solar radiation, surface net thermal radiation, 10 metre wind U component, 10 metre wind V component, 2 metre temperature, and 2 metre dewpoint temperature*. These were taken from the 060 and 18 UTC forecasts of the IFS experiments. The GloFAS model was run at 24 hour timesteps valid between 00-24 UTC, therefore the IFS values needed to be mapped onto each 24 hour timestep. For accumulated variables, such as total precipitation, surface and subsurface runoff, the 24 hour accumulations were created by combining data from the following forecast times [Table 1]:

Forecast Time	Lead Time (hours)
18 d <sub>1</sub>	6 - 12
06 d <sub>0</sub>	0 - 12
18 d <sub>0</sub>	0 - 6

*Table 1 24 hour accumulations at day 0 (d<sub>0</sub>) were created by combining IFS experiment data at the above forecast times*

For instantaneous variables, such as 2-metre temperature and the wind components, the average is taken across the instantaneous values at 00, 06, 12 and 18 UTC on the relevant day. All the forcings were regridded using nearest neighbour from the TCo399 grid onto the regular  $0.1^\circ \times 0.1^\circ$  grid [European Petroleum Survey Group - EPSG projection code 4326] used by GloFAS.

Daily streamflow outputs from GloFAS at  $0.1^\circ \times 0.1^\circ$  resolution valid for 0-24 hours lead time were used in the subsequent streamflow verification analysis. The streamflows represented the GloFAS forecast of discharge within the river component of each  $0.1^\circ \times 0.1^\circ$  model cell. This GloFAS setup was identical to a previous experiment which used ERA-5 for the hydro-meteorological forcings. The results from that particular experiment will be used later as proxy observations at the global level.

#### 4. Streamflow Verification Methodology

Results from the GloFAS streamflow experiments above were verified against in-situ observed streamflow values within Australia and the United States. These two countries were selected because of the good spatial coverage provided by their respective in-situ observations networks. Furthermore previous studies have suggested that SMOS soil moisture data have the greatest impact in these areas.

283 locations were chosen in the United States and 32 within Australia. These locations had been selected in a previous verification study of GloFAS [<http://www.globalfloods.eu/technical-information/glofas-30V2day/>] because they represented a range of different catchments found across the countries, as well as being at a spatial scale similar to that of GloFAS. It was necessary to shift the latitude and longitude coordinate of each in-situ location on to the nearest GloFAS river cell. This is because the  $0.1^\circ \times 0.1^\circ$  GloFAS channel network is a simplification of the real world channel locations, which can result in a small shift between the two. The shifting was done at each in-situ location by identifying the nearest channel cell in the GloFAS river network with a similar upstream area as the observed value. Additionally, a note was made at each in-situ about the extent of any anthropogenic intervention in the hydrological functioning of the river, for example if there were any dams or irrigation activity.

It was necessary to extract the in-situ streamflow observations from the respective monitoring agencies, as data for the time period of the GloFAS experiments was not already held. In Australia the data were extracted from the Bureau of Meteorology [BoM]. These were daily average streamflow observations which had been quality controlled. In the United States the data were extracted from the United States Geological Survey [USGS] and were six hourly average discharges. These were further averaged onto daily time steps, the units were converted from cubic feet per second to cubic metres per second. The

observed time series at each in-situ location was assessed for missing data, and locations with less than 90% completeness were eliminated from the subsequent analysis.

The estimated streamflow from the two GloFAS experiments were extracted at each in-situ location on each day during the experiment period. Each GloFAS experiment was compared against the respective observations by calculating the modified Kling-Gupta Efficiency [ $KGE_{mod}$ ] index [Gupta *et al.*, 2009; Kling *et al.*, 2012]. The  $KGE_{mod}$  is calculated as a combination of the correlation, the bias and the variability [Equation 1]:

$$KGE_{mod} = 1 - \sqrt{(r - 1)^2 + (\beta - 1)^2 + (\gamma - 1)^2}$$

$$r = \frac{cov_{s,o}}{\sigma_s \cdot \sigma_o}, \quad \beta = \frac{\mu_s}{\mu_o}, \quad \gamma = \frac{\sigma_s/\mu_s}{\sigma_o/\mu_o}$$

where  $r$  = correlation,  $\beta$  = bias,  $\gamma$  = variability,  $s$  = simulation [i.e. the GloFAS experiment],  $o$  = observation,  $cov$  = covariance,  $\sigma$  = the mean and  $\mu$  = standard deviation.

The  $KGE_{mod}$  is very useful for diagnosing the performance of a hydrological simulation as it combines three of the most important factors in producing good results. However great care must be taken if interpreting its results as a skill score owing to the lack of a benchmark predictor [Knoben *et al.*, 2019]. Therefore a skill score [Wilks, 2011] is computed to compare the  $KGE_{mod}$  results from the GloFAS simulations with and without SMOS soil moisture data assimilation [ $KGE_{mod}SS$ ]. Positive values will show where the GloFAS simulation which includes the assimilation of SMOS soil moisture data outperforms the simulation without the assimilation of SMOS.

$$KGE_{mod}SS = \frac{KGE_{mod}[with\ SMOS] - KGE_{mod}[without\ SMOS]}{KGE_{mod}Perf - KGE_{mod}[without\ SMOS]}$$

where  $KGE_{mod}Perf = 1$  which is a perfect score for the  $KGE_{mod}$ .

## 5. Verification Results

### 5.1. Verification against Observed Streamflow

#### 5.1.1. United States

A wide range of  $KGE_{mod}$  scores occur throughout the United States from the simulation with SMOS soil moisture data assimilation. A cluster of high values occur in the north west in the Colombia and upper Missouri basins, a cluster of low scores occurs in the Platte River in Nebraska [Figure 1a]. One explanation for the wide range of scores(?) could have been the presence of regulation within the river basins, a process which is only simplistically represented by GloFAS at some locations. However there is no apparent correlation between the  $KGE_{mod}$  value and whether a river is regulated. For example many of the locations with high  $KGE_{mod}$  scores in the north west are also regulated, whilst the Platte River is only marked in one location as being regulated [Figure 1a].

The  $KGE_{mod}$  skill scores are mostly centred around 0 [Figure 1b], meaning that there is little difference between the skill of the simulations with and without SMOS soil moisture data assimilation. The largest negative  $KGE_{mod}$  skill score values appear on the Platte River as well as the upper Nelson River in North Dakota. At these locations the  $KGE_{mod}$  values are less than zero in both GloFAS simulations with and without SMOS data assimilation. Analysing the hydrograph near the outlet of the Platte River shows that both GloFAS simulated hydrographs are much below the observed discharge [Figure 2]. The main difference between them is the discharge peak which occurs on the 1<sup>st</sup> November 2017. The peak is greater in the simulation when SMOS soil moisture is assimilated, but because this coincides with a trough in the observations this may be what causes the lower skill. Further analysis in the Platte River found that GloFAS simulates three reservoirs within this basin [at Kingsley, Seminoe and Pathfinder]. These could explain the low  $KGE_{mod}$  values in this basin as they may over-estimate the total reservoir storage and/or under-estimate the total outflow from one of, or all of, the reservoirs.

There were 40 locations where the  $KGE_{mod}$  skill score was 0.05 or more [Figure 1b], 31 of these locations had low  $KGE_{mod}$  values [less than 0.40], meaning that care must be taken when interpreting the apparent improvements at these locations. Two locations within the Wisconsin River demonstrated positive  $KGE_{mod}$  skill scores and  $KGE_{mod}$  values greater than 0.40. At one of these locations both GloFAS simulations capture the overall rise and fall within the observed discharge series, but neither capture the observed variability [Figure 2]. The GloFAS simulation which includes the assimilation of SMOS soil moisture has a large streamflow peak in May 2017 which better matches the observations, hence increasing the  $KGE_{mod}$ . However the peak is still not as sharply defined as in the observations [Figure 2].

Across all 283 gauging station locations in the United States the GloFAS simulation with SMOS soil moisture data assimilation shows slightly improved bias and  $KGE_{mod}$  values over the simulation without SMOS soil moisture data assimilation [Table 2]. A previous study [Verhoest *et al.*, 2015] also investigated the hydrological impact of SMOS data assimilation but within the upper Mississippi basin. Whilst that study did not explicitly analyse streamflow they found that CDF matching of modelled soil moisture from the VIC [Variable Infiltration Capacity] model to SMOS soil moisture resulted in higher values [Verhoest *et al.*, 2015]. This could explain the higher  $KGE_{mod}$  values observed at some locations in the GloFAS experiment which has SMOS soil moisture data assimilation. For example at the Wisconsin river [Figure 2] the higher streamflow in June 2017 in the GloFAS experiment with SMOS could be the result of higher soil moisture values leading to more generation of surface runoff.

	$R$	$Bias$	$KGE_{mod}$
<i>Without SMOS DA</i>	0.428	0.840	-0.504
<i>With SMOS DA</i>	0.420	0.812	-0.472

Table 2 Streamflow evaluation metrics averaged across the 283 United States gauging stations

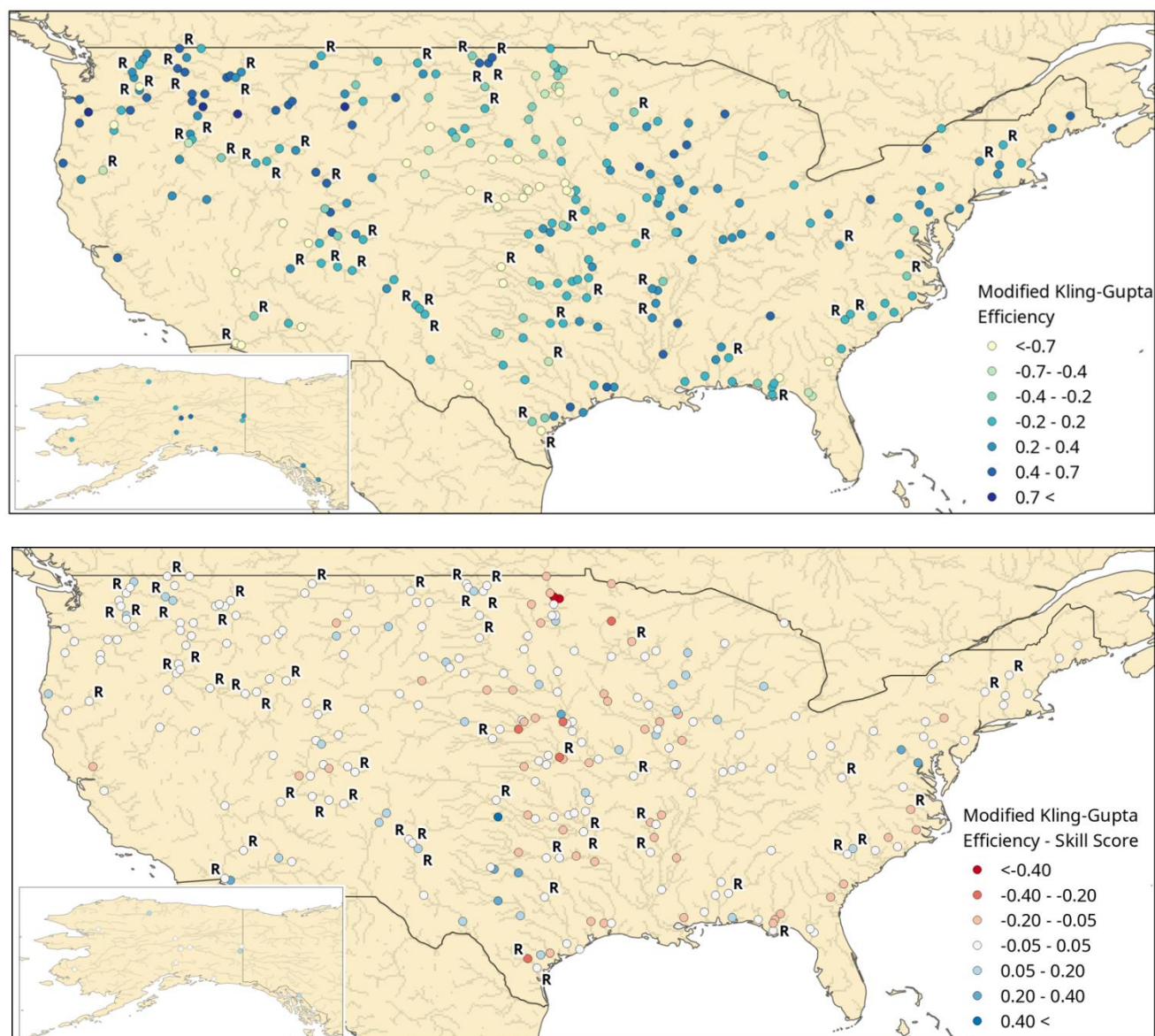


Figure 1 a) Modified Kling-Gupta Efficiency skill score calculated from GloFAS experiment with SMOS data assimilation against observed streamflow from the USGS. b) The skill score calculated with the  $KGE_{mod}$  from the GloFAS simulation with SMOS data assimilation referenced against the  $KGE_{mod}$  from the GloFAS simulation without SMOS data assimilation. The background shows the GloFAS channel network.

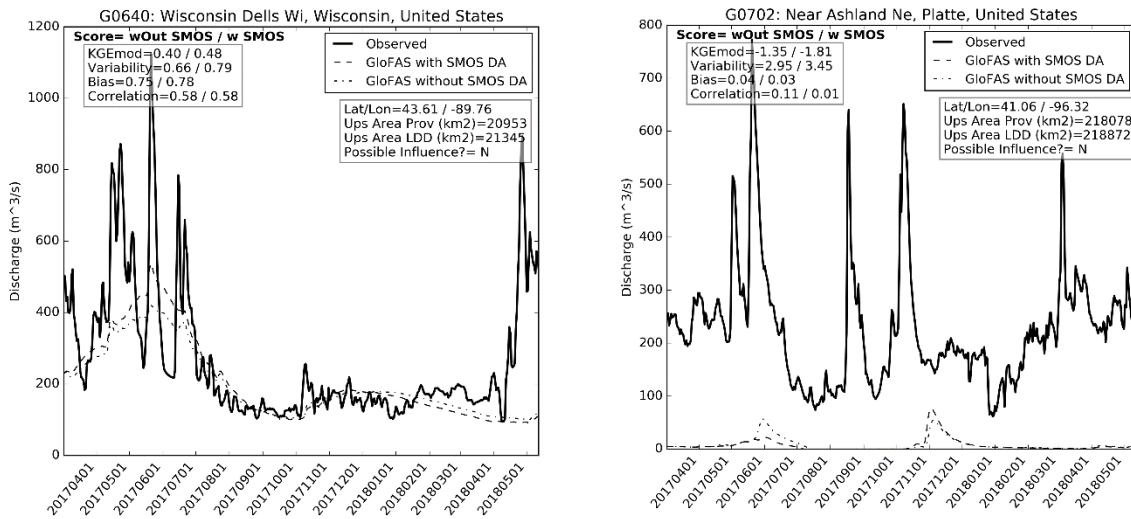


Figure 2 Hydrographs at the a) Wisconsin River, and b) Platte River

The  $KGE_{mod}$  from the simulation with SMOS data assimilation was broken down into its constituent components of: bias, variability and correlation [Figure 3]. This was done to explain the trends in the  $KGE_{mod}$  score above [Figure 1]. For the bias, values less than 1 show that GloFAS under-estimates streamflow with the reverse being true for values greater than 1. In this assessment GloFAS mostly has an under-estimation bias with some over-estimation in the south west [Figure 3]. The greatest under-estimation occurs within the Platte River, which as discussed above could be related to the treatment of reservoir storage within GloFAS [Figure 2]. The variability shows that GloFAS has a higher variability than the observations in locations where the  $KGE_{mod}$  score was low [Figure 3]. At the Platte River the higher GloFAS variability than the observations occurs because its baseflow meaning it is more sensitive to the peak flows which occur in June and November 2017 [Figure 2]. At the same location the GloFAS simulation with SMOS soil moisture data assimilation has a higher variability than the simulation without SMOS due to the greater November 2017 peak flow in the former simulation [Figure 2]. Correlation is greater than zero in most locations across the US, with 164 locations having a correlation greater than 0.4 [Figure 3]. Locations with the highest correlation also have higher  $KGE_{mod}$  scores. There is little difference in the correlation scores at these locations between the GloFAS simulations with and without SMOS soil moisture data assimilation [Figure 2].

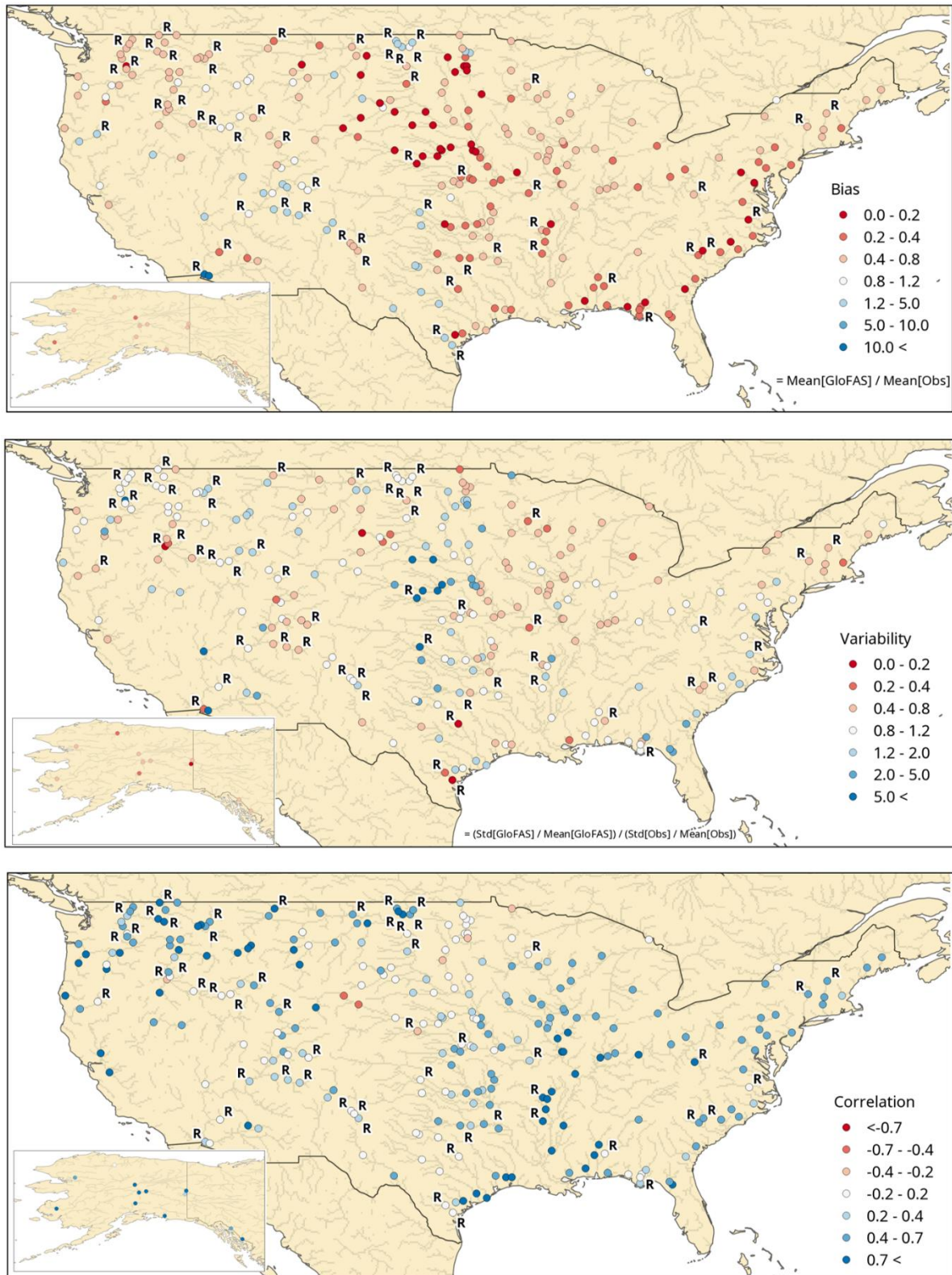


Figure 3 Constituents of the modified Kling-Gupta Efficiency skill score: a) bias, b) variability, and c) correlation. Calculated from the GloFAS experiment with SMOS data assimilation against USGS streamflow observations.

### 5.1.2. Australia

The  $KGE_{mod}$  values from the GloFAS simulation which includes SMOS soil moisture data assimilation show that values greater than 0.2 occur in the north of Australia [Figure 4]. For example in the Roper River both GloFAS simulations capture the peak streamflows between January to April 2018 [Figure 5]. Both GloFAS simulations miss the observed peak in April 2017, but both capture the extremely low baseflow from May 2017 to January 2018 which may be the main cause of the higher  $KGE_{mod}$  value at this location. The GloFAS simulation which includes SMOS soil moisture data assimilation has a lower peak flow in February 2018 than the GloFAS simulation without SMOS [Figure 5]. This better matches the observed peak flow at this time and may explain why the  $KGE_{mod}$  value improves from 0.57 to 0.65 when SMOS soil moisture data assimilation is included [Figure 5].

$KGE_{mod}$  values in the south east of Australia are mostly less than zero [Figure 4]a. The majority of these locations lie within the Murray Darling river basin which features a large amount of regulation to the natural river flow [Murray Darling Basin Authority, 2019]. Large quantities of water are extracted from the Murray Darling river for purposes including the irrigation of agricultural land, consequently observed streamflow would be lower than the original natural flow. The hydrographs near the outlet of the basin demonstrate this issue whereby both GloFAS simulations are greater than the observed streamflow [Figure 5]. Additionally the shape of both simulated GloFAS hydrographs does not match that of the observations. GloFAS includes three reservoirs within this basin but evidently these are insufficient to represent the full impact of the water management regime within the basin. At this location the GloFAS simulation with SMOS soil moisture data assimilation has lower peak flows than the GloFAS simulation without SMOS, something that also occurred in the north of the country [Figure 5].

The  $KGE_{mod}$  skill score in Australia shows a decline in  $KGE_{mod}$  scores in the north of the country and in the upper Murray-Darling basin when SMOS soil moisture data are assimilated [Figure 4]b. However in 9 locations the  $KGE_{mod}$  skill score is greater than 0.05, which shows an improvement when SMOS data are assimilated. All but two of these locations occur within the Murray Darling basin. The  $KGE_{mod}$  skill score values were often attributable to a difference in one or two flood peaks during the simulation period between the simulations with and without SMOS data assimilation. For example at the outlet of the Murray Darling basin the positive  $KGE_{mod}$  skill score value is due to the simulated peak in February 2018 being lower in the simulation which includes SMOS data assimilation which better matches the observation [Figure 5]. However for the rest of the simulation period the two simulations are almost identical. It is not clear what particular aspect of the SMOS soil moisture data assimilation might be causing these trends in the  $KGE_{mod}$  skill score. Care should be taken when interpreting the  $KGE_{mod}$  skill score trends in the Murray Darling basin however since neither GloFAS simulation captures the management processes.

Averaging the streamflow evaluation metrics across all 32 gauging stations shows a slight decline from the simulation which includes SMOS soil moisture data assimilation [Table 3]. Previous studies have also investigated the impact of SMOS data assimilation upon streamflow prediction in the Murray Darling basin using the VIC hydrological model [Lievens *et al.*, 2015 and 2016]. Their results found that SMOS data assimilation slightly improved the streamflow evaluation metrics, in contrast to the results found here. The differences between this study and those of Lievens *et al.*, 2015 and 2016 could be because this study looks across all of Australia, rather than just the Murray Darling basin.

Also, within the Murray Darling this study includes gauging locations near the outlet, whereas Lievens *et al.*, 2015 and 2016 focus on smaller catchments within the upper reaches. These smaller catchments may be less prone to water management processes which may be negatively affecting the streamflow metrics in this study.

	$R$	$Bias$	$KGE_{mod}$
<i>Without SMOS DA</i>	0.410	2.466	-1.248
<i>With SMOS DA</i>	0.356	2.558	-1.340

*Table 3 Streamflow evaluation metrics averaged across the 32 Australian gauging stations*

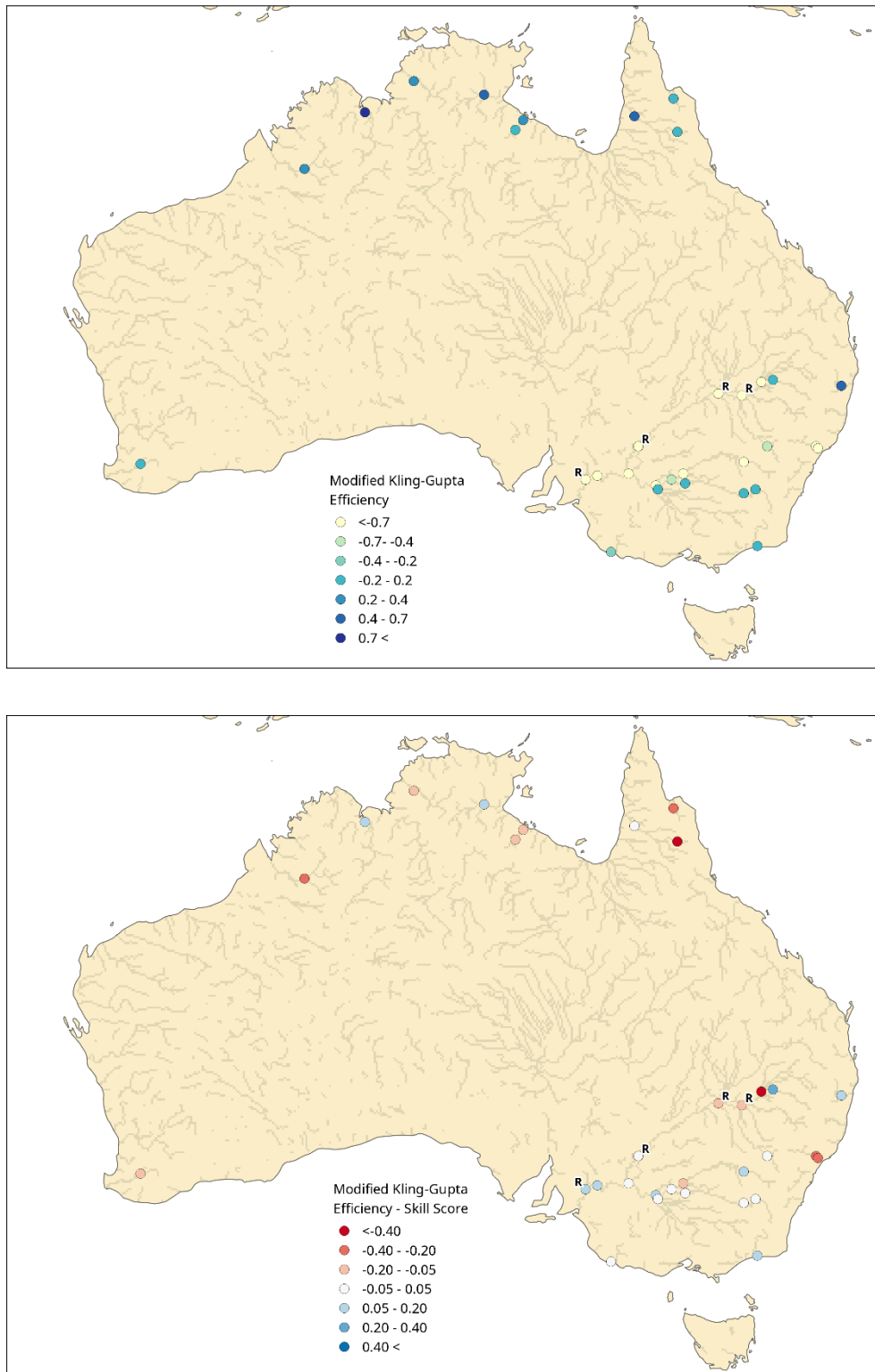


Figure 4 a) Modified Kling-Gupta Efficiency skill score calculated from GloFAS experiment with SMOS data assimilation against observed streamflow from the BoM. b) The skill score calculated with the  $KGE_{mod}$  from the GloFAS simulation with SMOS data assimilation referenced against the  $KGE_{mod}$  from the GloFAS simulation without SMOS data assimilation.

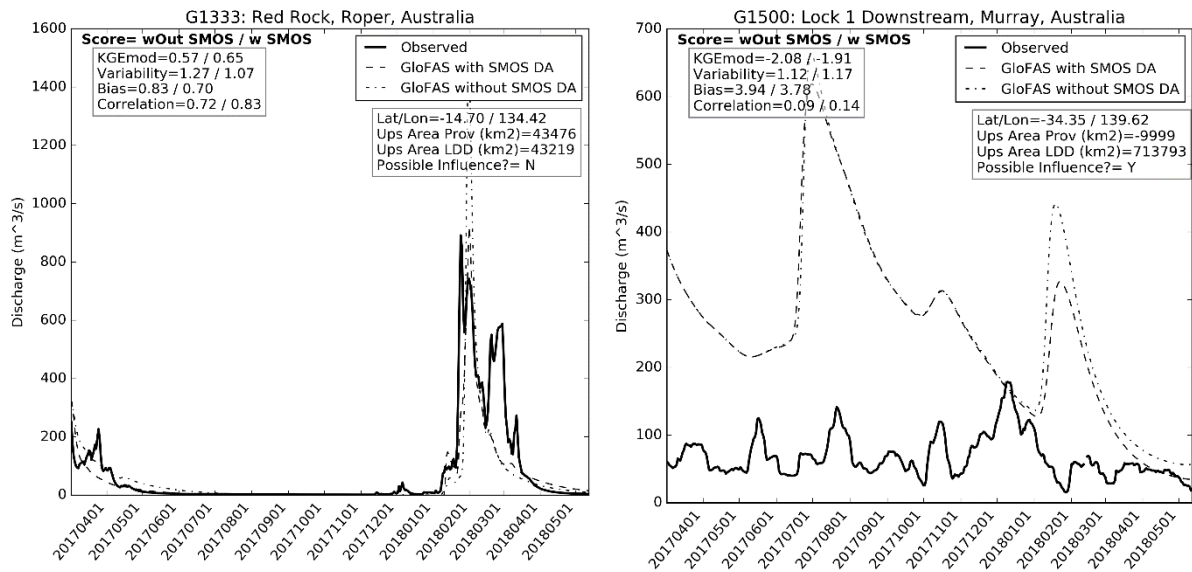


Figure 5 Observed and GloFAS simulated hydrographs at a) Roper River, Northern Australia and b) near the outlet of the Murray-Darling River.

The components of the  $KGE_{mod}$  show that the bias of the GloFAS simulation tends towards over-estimation, particularly within the Murray-Darling basin [Figure 6]. This is highlighted in the hydrograph at the outlet of the basin [Figure 5] and likely reflects the lack of GloFAS' ability to replicate the water management practices throughout the basin. For variability the GloFAS simulation under-estimates it in the north of the country and is slightly over-estimated in the Murray-Darling basin [Figure 6]. This could be due to GloFAS not under-estimating the magnitude of the flood peaks in the north of the country which would result in a lower standard deviation. In the Murray-Darling this is because the river management practices, not represented in GloFAS, aim to reduce the variability of the stream-flow. The correlation is highest in the north of the country where river flows are more natural than in the Murray-Darling basin where the correlation is lower [Figure 6].

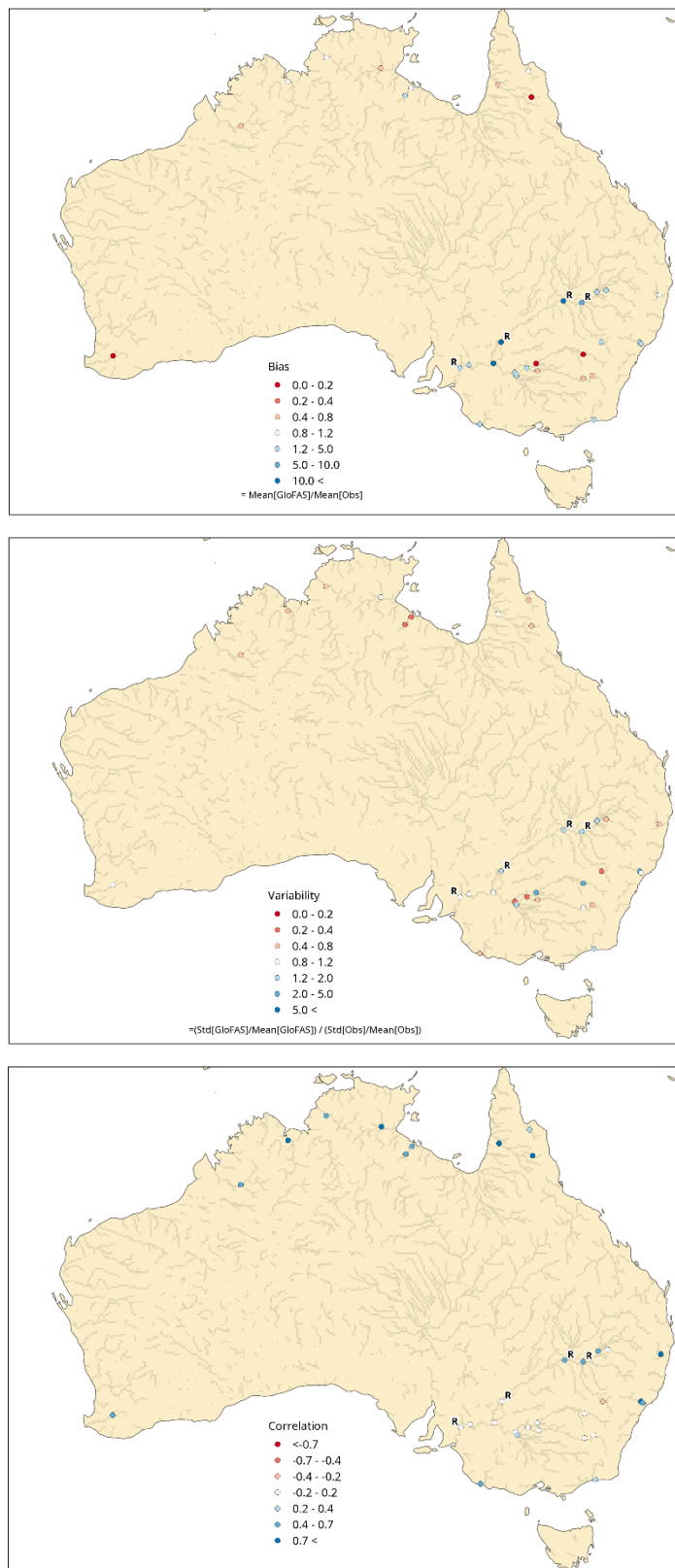


Figure 6 Constituents of the modified Kling-Gupta Efficiency skill score: a) bias, b) variability, and c) correlation. Calculated from the GloFAS experiment with SMOS data assimilation against BoM streamflow observations.

## 5.2. Verification against GloFAS ERA-5 Simulation

The previous analysis of GloFAS simulated streamflows against observations was hindered by the presence of regulation in many of the basins. Since these regulations are very difficult to simulate within GloFAS owing to the lack of process representation, it meant that it was difficult to assess whether the results in the performance metrics were due to the influence of SMOS soil moisture data assimilation or the river regulation. Furthermore the significant effort required to extract and process the streamflow observations meant it was only possible to perform the analysis in the United States and Australia. In this section a secondary analysis is performed globally but using a GloFAS simulation forced with ERA-5 re-analysis data as a proxy for observed streamflow.

The GloFAS ERA-5 simulation was produced in a previous study by forcing the LISFLOOD river routing procedure with the IFS variables described in section 3 but derived from ERA-5.

The Mean Absolute Error [MAE] was computed from the river discharge for the GloFAS simulations with and without SMOS soil moisture data assimilation against the GloFAS ERA-5 simulation.

$$MAE = \frac{\sum_{i=1}^n |GloFAS_{SMOS\ i} - GloFAS_{ERA-5\ i}|}{n}$$

where  $n$  = number of data points which in this case is the number of days during the simulation period. The MAE will show the average absolute difference between both GloFAS SMOS experiments and the GloFAS ERA-5 simulation. The metric was chosen instead of the  $KGE_{mod}$  because the proxy observation dataset in this particular instance, from the GloFAS ERA-5 simulation, will have similar biases to the GloFAS SMOS experiments as they are produced by the same hydrological model. Therefore it would be unnecessary to analyse some of the components of the  $KGE_{mod}$ . Instead the MAE provides a simpler approach more suitable for this particular analysis.

The units of the MAE will be in  $m^3s^{-1}$  which is the same as the units of the GloFAS discharge simulations. However this will mean that the catchment area will influence the results. To avoid this the streamflows were converted into specific discharge, whereby they are divided by their upstream area, and the MAE was computed from these.

Results show that the greatest MAE values lie within a latitude band of  $22^\circ$  -  $-10^\circ$  within the tropics [Figure 7]. Within this band the upper reaches of the Nile, Congo and Amazon rivers have some of the largest MAE values. High values are also found in the Indonesian archipelago, south east Asia, the Himalayas, the west coast of Africa and southern Mexico [Figure 7].

To calculate the impact of the SMOS soil moisture data assimilation, the difference in the specific discharge MAE from the GloFAS simulations with and without the data assimilation was calculated. Results show that the MAE from the GloFAS simulation with SMOS data assimilation is most frequently smaller than that from the GloFAS simulation without SMOS data assimilation [Figure 8]. However there are areas where the reverse is true, for example in North America especially around the Hudson Bay. The greatest differences, of whichever sign, are in the same locations as those which have the greatest MAE values [Figure 7].

It is not clear why the differences in the MAE values between the two GloFAS SMOS simulations emerge. It may be that one of the simulations has higher flows than the other for example. To investigate this the differences in the 5<sup>th</sup> and 95<sup>th</sup> percentiles of the specific discharges [representing low and high flows respectively] were computed. The 5<sup>th</sup> percentile shows the greatest differences within the

same tropical latitude band as for the MAE [Figure 9]. In the upper Brazilian/Columbian Amazon basin the 5<sup>th</sup> percentile specific discharges from the GloFAS simulation with SMOS data assimilation are lower than those from the GloFAS simulation without SMOS data assimilation. Whereas in the Bolivian Amazon the reverse is true. No clear trend in the 5<sup>th</sup> percentile differences is in evidence in the Indonesian archipelago, as values of opposing sign occur next to each other. In North America in the tributaries of the Mississippi basin 5<sup>th</sup> percentile specific discharges are slightly lower in the GloFAS simulation with SMOS data assimilation. Whilst in north west America and most of Canada the GloFAS simulation with SMOS data assimilation has higher 5<sup>th</sup> percentile specific discharges. Differences are more globally widespread in the 95<sup>th</sup> percentile specific discharges between the two GloFAS SMOS data assimilation experiments [Figure 10]. The greatest differences are within the Amazon basin, western Africa and the India/Bangladesh/Myanmar area. Weaker differences occur in eastern China, the Indonesian archipelago, South America, central Africa, northern Australia and northern Russia [Figure 10]. However there is no clear spatial trend to these differences, as differences of opposing sign occur close to each other.

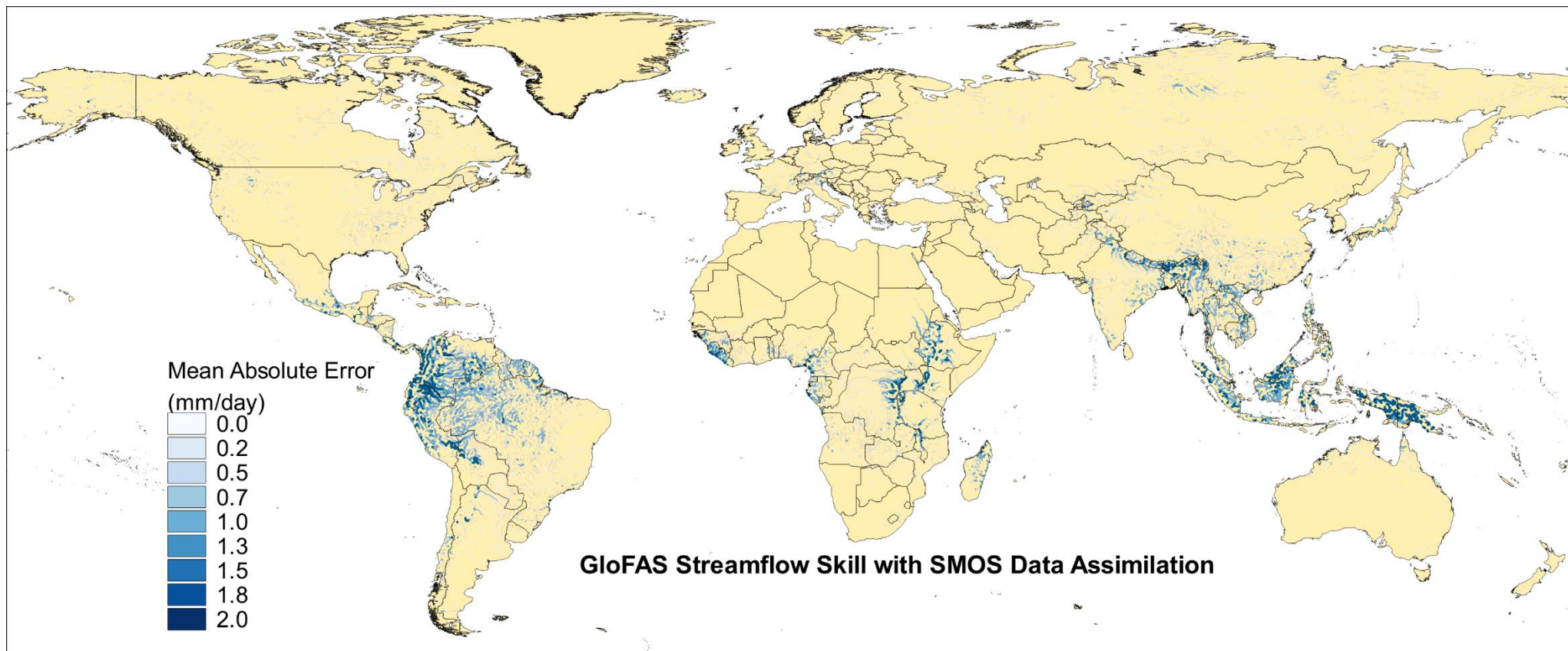


Figure 7 Mean absolute error of GloFAS specific discharge compared against the GloFAS ERA-5 re-analysis simulation.

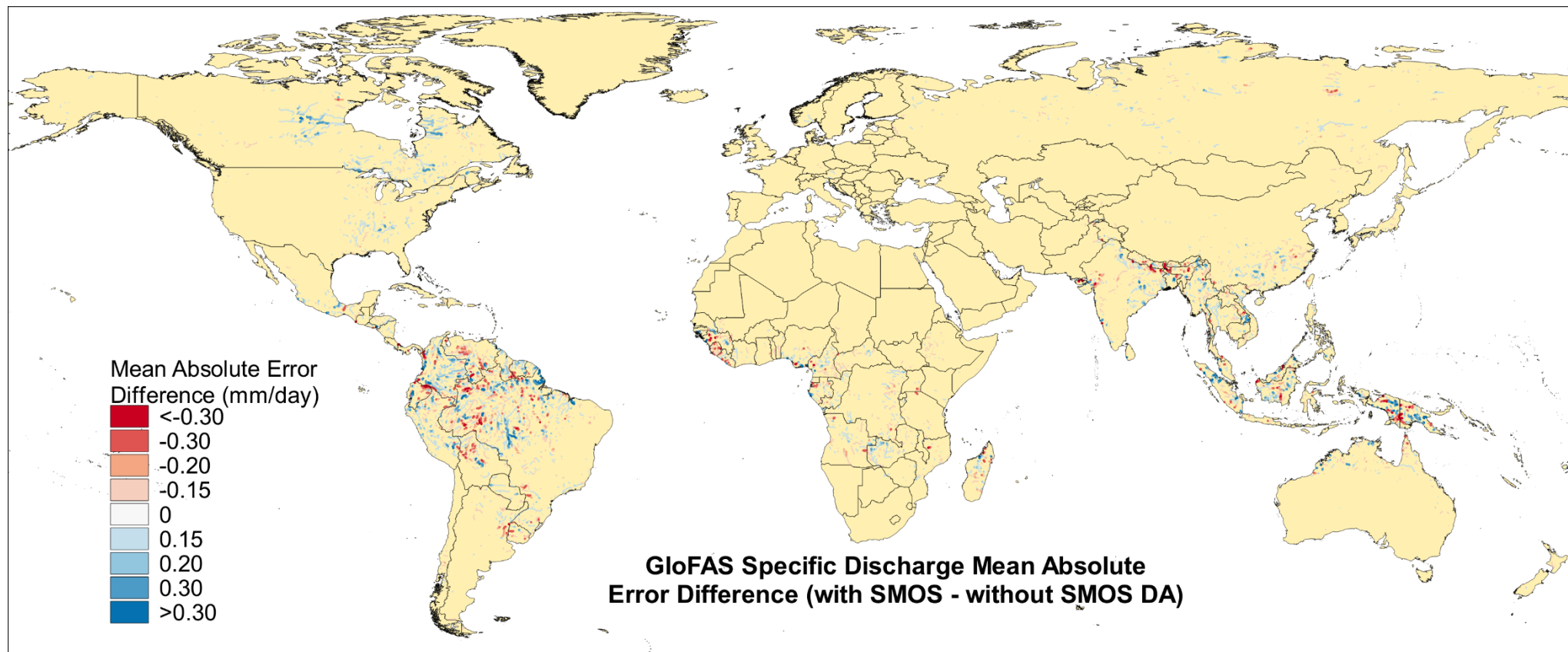


Figure 8 Difference in Mean Absolute Error skill score of specific discharge from the GloFAS simulations with and without SMOS data assimilation, when compared against the GloFAS ERA-5 re-analysis. Red shows an improvement in MAE with SMOS data assimilation, blue shows a decline.

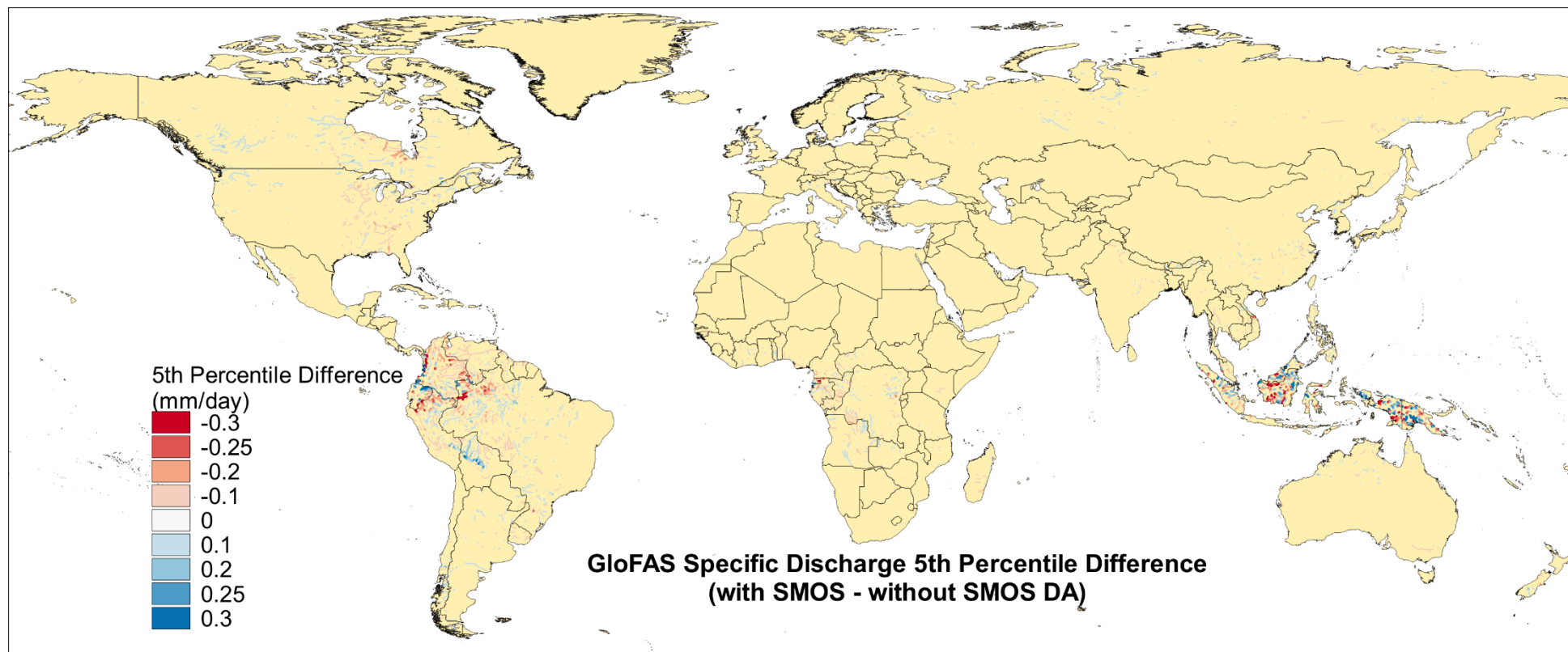


Figure 9 Difference in the 5<sup>th</sup> percentile (low flow) of specific discharge from the GloFAS simulations with and without SMOS data assimilation.

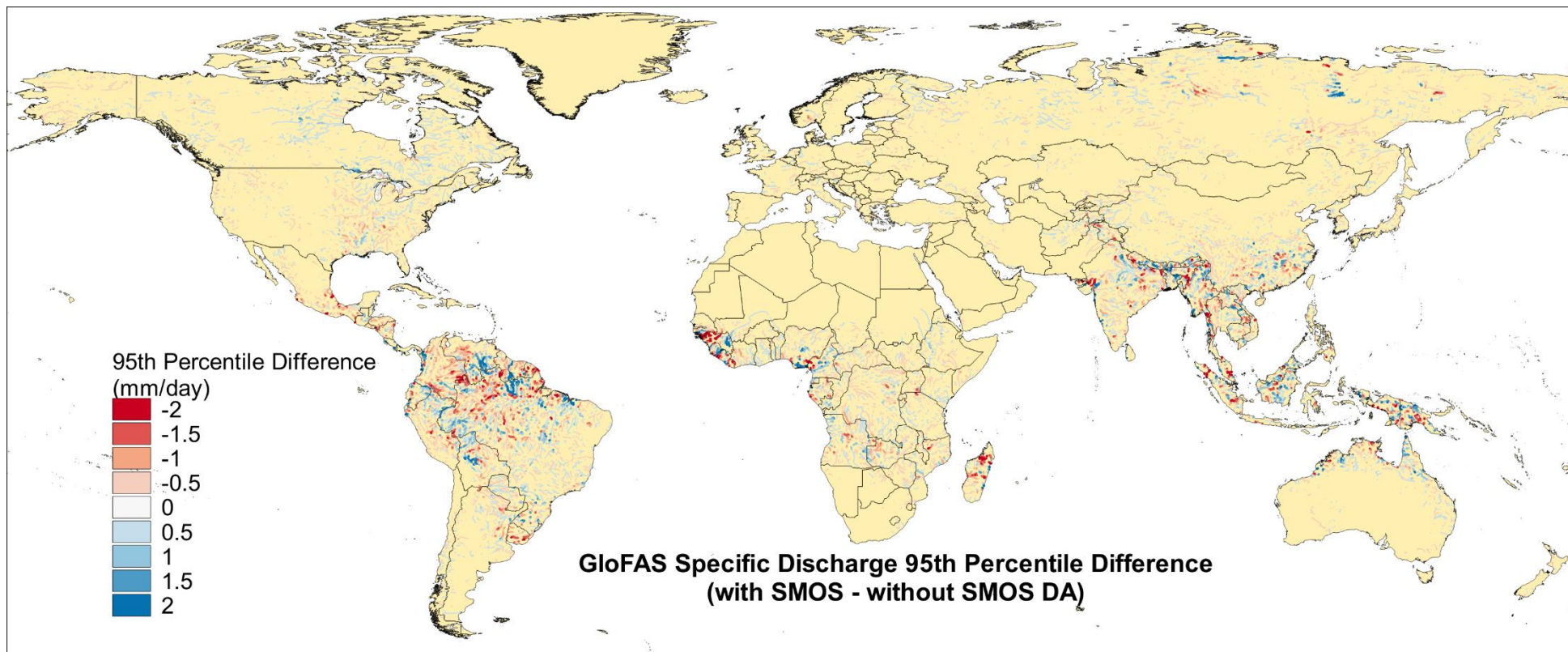


Figure 10 Difference in the 95th percentile (high flow) of specific discharge from the GloFAS simulations with and without SMOS data assimilation.

## 6. Discussion & Conclusions

One point for discussion is the use of a calibrated hydrological model to perform the streamflow predictions. As mentioned above, GloFAS was calibrated in a previous study by optimizing the streamflow parameters using forcings from a 20 year ECMWF reforecast [Hirpa *et al.*, 2018]. The calibration of a given hydrological model can sometimes mean that it is difficult for any subsequent simulation to outperform it. However the GloFAS calibration study only tuned the streamflow parameters and left the vertical hydrological component, i.e. HTESSSEL, unchanged. Hence it is still possible to improve the performance of this latter component, for example with the assimilation of SMOS soil moisture data within the forcings. This is evidenced by the improvements observed at some locations in the United States whereby peak discharges better matched the observations after the assimilation of SMOS soil moisture [Figure 2]. Increased soil moisture values from the assimilation of SMOS soil moisture, as suggested in Verhoest *et al.*, 2015, could cause increased surface runoff production and hence greater streamflows.

Another point to consider is the implicit bias correction within the SMOS soil moisture product that was used in this study. The SMOS product was created by applying a neural network procedure which was trained on ECMWF soil moisture data. This procedure would implicitly remove any biases between the SMOS observations and the ECMWF model. However this would restrict the data assimilation to only correcting for random model errors rather than also correcting the bias, preventing it from changing the behavior of the soil moisture [Lievens *et al.*, 2016]. Assimilating the SMOS neural network product trained on the SMOS level 2 soil moisture data could offer a solution, as this product is not bias corrected to the ECMWF model. However it would not currently work within the ECMWF data assimilation system as it breaks the assumption of zero observation-model bias. A possible solution for future work would be to perform a parameter analysis of HTESSSEL which may involve tuning its parameters which control the vertical soil water budget.

Overall in this study two GloFAS experiments have been conducted using hydro-meteorological forcings from the IFS experiments which include and exclude the assimilation of SMOS soil moisture data. Streamflow predictions from both GloFAS experiments have been evaluated against observations either from in-situ measurements or from a GloFAS ERA-5 simulation using the  $KGE_{mod}$  and MAE metrics respectively. The  $KGE_{mod}$  skill score was calculated to show where hydrological skill could have been improved by the assimilation of SMOS soil moisture and the difference in the MAE values between the two experiments was calculated for the same purpose. The results showed no clear spatial trend to any changes in hydrological skill which emerged. The greatest changes between the simulations occur within the tropical latitude band. Outside of this the changes between the simulations were smaller.

Further investigation was made as to how the hydrological skill of the two GloFAS simulations changed by analysing the impacts upon low and high flows. There was no clear spatial trend to these changes either. Investigating the hydrographs at specific station locations found that differences in  $KGE_{mod}$  could often be attributed to differences in a single flood peak, whilst the remainder of the simulated hydrographs were identical. In some instances the flood peak in the simulation with SMOS data assimilation was the greatest, whilst the opposite was true in other instances. This suggests that future work should focus on finding out how the SMOS data are affecting the GloFAS simulations. Rather than looking over an entire simulation period it should focus upon a specific flood event where SMOS

data are available. It could then look at the increments between the first guess and the analysis. This would show the impact of SMOS soil moisture data assimilation upon the HTESSSEL soil moisture and if it correlates to differences in the GloFAS simulations. Globally this analysis could be expanded by analyzing the correlation between the soil moisture increments resulting from SMOS and the differences in the GloFAS streamflow simulations.

## Acknowledgements

This work was funded under the ESA-ESRIN contract number 4000125399/18/I-BG for the SMOS-emergency services [SMOS-E] project. Ruth Coughlan provided valuable assistance with the retrieval of streamflow observation data in the United States and Australia. Shaun Harrigan gave very useful advice regarding the interpretation and visualisation of the  $KGE_{mod}$  score.

## References

- Bollrich, G. 1992. *Technische Hydromechanik: Grundlagen*. Wissen. Verlag Bauwesen
- ECMWF. 2018. IFS Documentation - Cy45r1 Operational implementation 5 June 2018. Part IV: Physical Processes. Reading, 223pp, <https://www.ecmwf.int/node/18714>
- de Rosnay P., M. Drusch, D. Vasiljevic, G. Balsamo, C. Albergel and L. Isaksen: A simplified Extended Kalman Filter for the global operational soil moisture analysis at ECMWF, *Q. J. R. Meteorol. Soc.*, 139:1199-1213, 2013
- de Rosnay, P. and N. Rodríguez-Fernández, D. Fairbairn, J. Muñoz-Sabater, H. Lawrence, C. Baugh, F. Di Giuseppe, S. English, C. Prudhomme, M. Drusch, S. Mecklenburg, oral (invited): "SMOS Soil Moisture Data Assimilation for Operational Numerical Weather Prediction"
- Gupta, H.V., Kling, H., Yilmaz, K.K., Martinez, G.F. 2009. Decomposition of the mean squared error and NSE performance criteria: Implications for improving hydrological modelling. *Journal of Hydrology* 377(1-2), pp. 80-91. <https://doi.org/10.1016/j.jhydrol.2009.08.003>
- Hirpa, F.A., Salamon, P., Beck, H.E., Lorini, V., Alfieri, L., Zsoter, E., Dadson, S.J. 2018. Calibration of the Global Flood Awareness System (GloFAS) using daily streamflow data. *Journal of Hydrology* 566, pp. 595-606. <https://doi.org/10.1016/j.jhydrol.2018.09.052>
- Kling, H., Fuchs, M., Paulin, M. 2012. Runoff conditions in the upper Danube basin under an ensemble of climate change scenarios. *Journal of Hydrology* 424-425, pp. 264-277. <https://doi.org/10.1016/j.jhydrol.2012.01.011>
- Knoben, W.J.M, Freer, J.E., Woods, R.A. (2019), Technical Note: Inherent benchmark or not?: Comparing Nash-Sutcliffe and Kling-Gupta efficiency scores, *Hydrology and Earth System Sciences Discussions*, <https://doi.org/10.5194/hess-2019-327>.
- Lehner, B., Verdin, K., Jarvis, A. 2008. New global hydrography derived from spaceborne elevation data. *Eos Transactions*, AGU 89(10): pp 93-94

- Lievens, H., Tomer, S.K., Al Bitar, A., de Lannoy, G.J.M., Drusch, M., Dumedah, G., Hendricks Franssen, H.-J., Kerr, Y.H., Martens, B., Pan, M., Roundy, J.K., Vereecken, H., Walker, J.P., Wood, E.F., Verhoest, N.E.C., Pauwels, V.R.N. 2015. SMOS soil moisture assimilation for improved hydrologic simulation in the Murray Darling Basin, Australia. *Remote Sensing of Environment* 16, pp. 146-162. <https://doi.org/10.1016/j.rse.2015.06.025>
- Lievens, H., de Lannoy, G.J.M., Al Bitar, A., Drusch, M., Dumedah, G., Hendricks Franssen, H.-J., Kerr, Y.H., Tomer, S.K., Martens, B., Merlin, O., Pan, M., Roundy, J.K., Vereecken, H., Walker, J.P., Wood, E.F., Verhoest, N.E.C., Pauwels, V.R.N. 2016. Assimilation of SMOS soil moisture and brightness temperature products into a land surface model. *Remote Sensing of Environment* 180, pp. 292-304. <https://doi.org/10.1016/j.rse.2015.10.033>
- Murray Darling Basin Authority. 2019. Basin Plan Annual Report 2017-2018. December 2018. Publication number 01/19, 32 pp. <https://www.mdba.gov.au/sites/default/files/pubs/basin-plan-annual-report-2017-18.pdf>
- Rodriguez-Fernandez, N., de Rosnay P., Albergel C., Richaume P., Aires F., Prigent C., Kerr Y.: "SMOS Neural Network Soil Moisture Data Assimilation in a Land Surface Model and Atmospheric Impact", *Remote Sensing*, 11(11), 1334, 2019
- van der Knijff, J.M., Younis, J., de Roo, A.P.J. 2010. LISFLOOD: a GIS-based distributed model for river basin scale water balance and flood simulation. *International Journal of Geographical Information Science* 24(2), pp189-212. <https://doi.org/10.1080/13658810802549154>
- Verhoest, N.E.C., van den Berg, M.J., Martens, B., Lievens, H., Wood, E.F., Pan, M., Kerr, Y.H., Al Bitar, A., Tomer, S.K., Drusch, M., Vernieuwe, H., de Baets, B., Walker, J.P., Dumedah, G., Pauwels, V.R.N. 2015. Copula-based downscaling of coarse-scale soil moisture observations with implicit bias correction. *IEEE Transactions on Geosciences and Remote Sensing* 53(6), pp. 3507-3521. <https://doi.org/10.1109/TGRS.2014.2378913>
- Wilks, D.S. 2011, *Statistical Methods in the Atmospheric Sciences*. Third Edition. Academic Press. Oxford.
- Wu, H., Kimball, J.S., Li, H., Huang, M., Leung, L.R., Adler, R.F. 2012. A new global river network database for macroscale hydrologic modelling. *Water Resources Research* 48, W09701. <https://doi.org/10.1029/2012WR012313,%202012>
- Yamazaki, D., O'Loughlin, F., Trigg, M.A., Miller, Z.F., Pavelsky, T.M., Bates, P.D. 2014. Development of the Global Width Database for Large Rivers. *Water Resources Research* 50(4), pp. 3467-3480. <https://doi.org/10.1002/2013WR014664>
- Zajac, Z., Revilla-Romero, B., Salamon, P., Burek, P., Hirpa, F., Beck, H. 2017. The impact of lake and reservoir parameterisation on global streamflow simulation. *Journal of Hydrology* 548: pp. 552-568. <https://doi.org/10.1016/j.jhydrol.2017.03.022>